©2019 Published in 7th International Symposium on Innovative Technologies in Engineering and Science 22-24 November 2019 (ISITES2019 SanliUrfa - Turkey)
https://doi.org/10.33793/acperpro.02.03.127

Experimental Investigation of Flow Structures Around side-by-side Yawed Cylinders in Shallow Water

[1]Ebubekir KÜTÜK, [1]Umutcan OLMUŞ, [2]Tahir DURHASAN, *[1]Hüseyin AKILLI,
*[1]Faculty of Engineering and Architecture, Department of Mechanical Engineering, Çukurova University, 01130 Adana/Turkey
[2]Faculty of Aeronautics and Astronautics, Department of Aerospace Engineering, Adana Alparslan Türkeş Science And Technology University, 01250 Adana/Turkey

Abstract

The aim of this experimental study is to investigate the flow behaviour around two equally yawed side-by-side cylinders in shallow water. Time averaged velocity vector fields, Reynolds shear stress distrubutions and streamline patterns were obtained using Particle Image Velocimetry (PIV) technique. The gap ratio between the cylinders were in the range of G/D=0.25-1.25 with an increment of 0.25 where G is the distance between the cylinders and D is the cylinder diameter. Five different yaw angles of cylinders were employed during the experiment. The results showed that the yaw angle, α had an important effect on the flow structures of the downstream of the cylinders. Reynolds shear stress and vortex structures were decreased, the intensity of the jet like flow were significantly attenuated for the gap ratios of G/D=0.25, 0.50 and 0.75.

Key words: Shallow water, side-by-side cylinders, yawed cylinders

1. Introduction

Two circular cylinders in the side by side arrangements have been using broadly in the many engineering applications such as oil and gas platforms, bridge piers, buildings, power transmission lines, heat exchangers, offshore and on land structures. Therefore investigation of flow around side-by-side cylinders has been drawing interest by researchers [3,5,17,18].

Bearman and Wadcock [4] studied quasi-stable behaviour and flopping for a two-cylinder array as a function of cylinder spacing. Peschard and Le Gal [9] observed the interaction of wakes downstream of a two-cylinder array with $2 \leq T/D \leq 7$ and $90 \leq ReD \leq 150$. Although they successfully model quasi-stable behavior, no spontaneous or forced flopping was observed. Williamson [16] studied evolution of a single wake behind a pair of bluff bodies.

*Corresponding author: Address: Faculty of Engineering and Architecture, Department of Mechanical Engineering, Çukurova University, 01130 Adana/Turkey. E-mail address: hakilli@cu.edu.tr, Phone: +903223386084

He showed that following antiphase vortex shedding at the cylinders, the downstream is indeed two parallel streets in antiphase. In the case of in-phase vortex shedding the configuration of two in-phase parallel streets does not ocur except for a small region behind the cylinders. He found that the wakes from each cylinder combine to form a single large scale wake as a binary vortex street. Furthermore he indicated that even for smaller gaps when the flow is distincly asymmetric, there are certain modes of vortex shedding. Wei and Chang [15] studied turbulence effect on the interaction of wake and base-bleed flow downstream of two circular cylinders arranged side-by-side. They found that free stream turbulence was effective on the wake flow behavior. However, the biasing characteristic of the gap flow was not substantially affected by free stream turbulence. Sumner et al. [12] measured the flow patterns behind two and three side-by side circular cylinders in the range of G/D=1∼6 and ReD =500-3000 using flow visualization and particle image velocimetry techniques (PIV). They noted considerable variation in the flow patterns at a given G/D.

In shallow flow conditions surface effects and bottom frictions show important effects on the flow characteristics. A shallow flow is one in which the horizontal dimensions are much larger than the vertical extent and the vertical component of water particle acceleration components so that the pressure variation can be assume hydrostatic. Shallow flows has been also investigated by researchers. Akıllı et al. [1] investigated experimentally the flow around two and three side-by-side circular cylinders of equal diameter (ReD=5000) in shallow water using the particle image Velocimetry (PIV) technique, over a transverse gap ratio in the range of G/D= 1.0-3.0 with an increment of 0.25. For the two side-by-side cylinder case, they found that the flow structure behind the cylinders is asymmetrical at small gap ratios as a result of jet-like flow between the cylinders. The jet-like flow tends to deflect toward the near wake region that has a higher vortex shedding frequency. In the case of three cylinders, they observed both an asymmetrical flow structure at small gap ratio (G/D= 1.25) and a symmetrical flow structure at intermediate gap ratios (1.5<G/D<2.0). They also observed occurance of bistable wake regions for the asymmetrical cases. Oruc et al. [11] carried out an experiment of suppression of asymmetric flow behaviour downstream of two side-by-side circular cylinders with a splitter plate in shallow water. They found that using of splitter plate should be a favorable method to control the asymmetric flow behavior downstream of two side-by-side arranged circular cylinders for L/D = 3 or L/D = 4. Ingram and Chu [8] studied different instability mechanisms in the shallow water flow and defined a dimensionless wake stability parameter S to account for the stabilizing effect of the transverse shear. The parameter S which is based on the ratio of the small-scale kinetic energy loss to the production of large-scale turbulent kinetic energy is defined as S =C_fD/h for the bluff body, where C_f is the bottom friction coefficient, D is the width or diameter of a bluffbody, and h is the water depth. Akilli and Rockwell [2] studied vortex formation from a cylinder in shallow water using a combination of visualization marker and particle image velocimetry technique (PIV). At the bed, the time-averaged streamline topology downstream of the base of the cylinder takes on a form known as owl face of the first kind, which was originally defined for a completely different exterior flow. As mentioned above, it is evident that most of the experimental studies were concentrated on the behaviors of gap flow through two side-by-side cylinders that are vertically oriented to the flow direction. On the other side, in the engineering applications, the cylindirical structures such as piers, off shore oil and gas platforms are commonly yawed structures. Several investigations on flow past a single yawed cylinder have been investigated. Vakil and Green [14] studied drag and lift coefficients of inclined finite circular cylinders at moderate Reynolds number. They indicated that the Indipendence Principle is not accurate for α≤45º. They also found that for all aspect ratios the

ratio of the lift and drag forces reaches a maximum for $40^o < \alpha < 50^o$. Thapa et al. [13] performed three-dimensional simulations of vortex shedding flow in the wake of yawed circular cylinder near a plane boundary and they found that increasing the cylinder yaw angle, weakens three dimensionality of the flow. Franzini et al. [6] performed flow around a stationary and yawed cylinder under asymmetrical end conditions. They reported that when the cylinder angle reached to 45^o, there was no regular vortex-shedding regime. Hogan and Hall [7] experimentally illustrated that increasing the yaw angle of the cylinder to the mean flow direction causes the vortex shedding in the wake to become more disorderly. Liang et al. [10] numerically studied spanwise characteristics of flow crossing a yawed circular cylinder of finite length. They reported that the Karman vortex Street is almost breakdown especially in the region near the upstream end-plate.

The studies published above by the researchers show that there is no extensively investigation in yawed circular cyilnders in side by side arrangements in the shallow water conditions. Therefore, the aim of present work is to obtain flow charactarestics and effects of yaw angles on the flow behaviours on the downstream region of the two identical yawed circular cylinders in shallow water using PIV technique. The experiments were carried out in the range $0.25 \leq G/D \leq 1.25$ with an increment of 0.25. The laser sheet was located parallel to the bottom of the water channel at the mid-level of the water height.

2. Experimental Set Up

Experiments were performed in a large-scale water channel located in the Fluid Mechanical Laboratory of the Department of Mechanical Engineering at Çukurova University. The water channel (see Figure 1) test section which has of 8000mmx1000mmx750mm was constructed from a 15 mm thick transparent plexiglass sheet with upstream and downstream fiberglass reservoirs. Water flow speeds were controlled by a centrifugal flow pump. Before reaching the test chamber, the water was pumped into a settling chamber and passed through a honeycomb section and two-to-one channel contraction. For side by side configurations a long polyethelene block prepared with desired holes (diameter of 51mm) which were spaced center-to-center as arranged parameters.

A schematic view of the test section mounted in the water channel shown in Figure 2. During all experiment, the water level was (h_w) maintained with the depth of 50 mm which equals to the cylinder diameter D=50mm. In the present study, following points were studied: Analysing and observing of the flow structure behind the cylinders and the effects of yaw angles α, arrangement of side by side configurations. The freestream velocity U_∞ =214mm/s which corresponds to the Reynolds number Re_D=10700 using particle image velocimetry (PIV) technique. $Re=U_\infty D/\nu$, based on the cylinder diameter. Here, ν is the kinematics viscosity, D is the cylinder diameter and U_∞ is the free-stream velocity. The plexiglass pipes (or named cylinder) were used as test models. Five different yaw angles of cylinders α=0º, 15º, 20º, 30º, 45º were used in the experiments. The distance between the cylinders, G, was changed in the range of $0.25 \leq G/D \leq 1.25$ with an increment of 0.25. Here, G is the distance between two cylinders, D is the cylinder diameter.

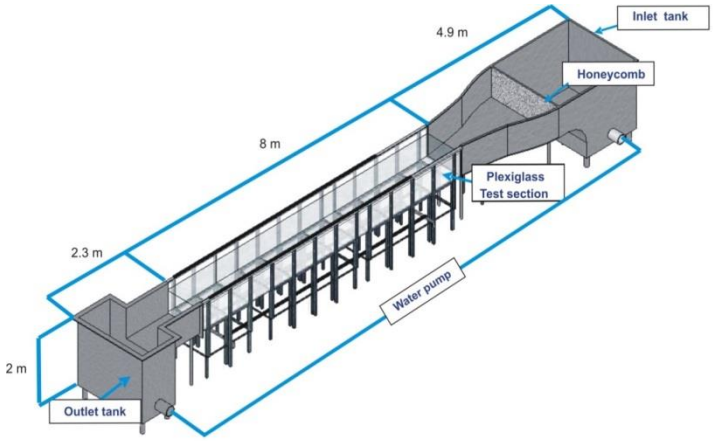

Figure 1. Schematic representation of water channel

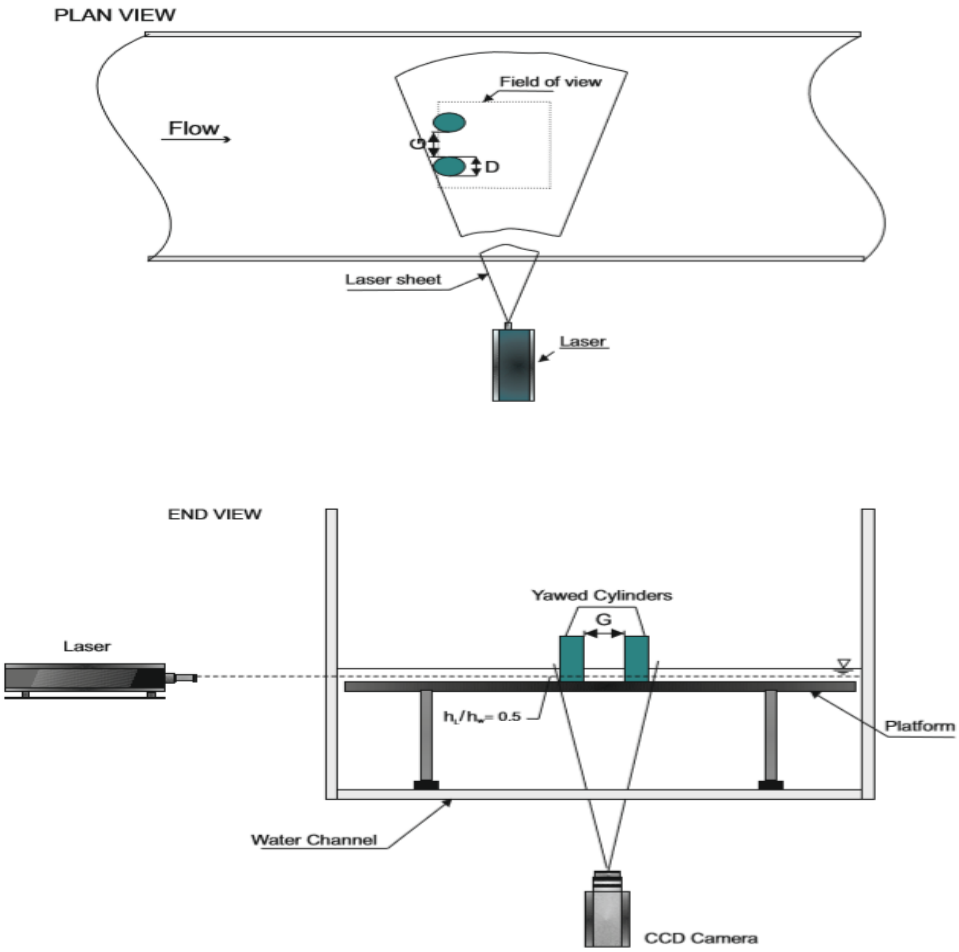

Figure 2. Schematic of the experimental system and definition of parameters for Side-by-side yawed cylinders configurations

The PIV experiments were conducted in plan-view. The measurement field was illuminated by a thin and an intense laser light sheet by using a pair of double-pulsed Nd: YAG (yttrium aluminum garnet) laser units (Figure 2.) each having a maximum energy output of 120mJ at 532nm wavelength. The laser sheet was oriented parallel to the bottom surface of the water channel and the experiments were carried out at midsection of the water height. The image capturing was performed by an 8-bit cross-correlation CCD (Charge Coupled Device) camera (Figure 2.) having a resolution of 1600 x 1200 pixels, equipped with a lens of focal length 60 mm and 105 mm. In the image processing, 32×32 rectangular interrogation pixels were used and an overlap of 50% was employed.

The time interval between pulses was 1.75 ms for all experiments and the thickness of the laser sheet illuminating the measurement plane was approximately 2mm. The time interval and the laser sheet thickness were selected such that the maximum amount of particles in the interrogation window was obtained. A total of 7326 (99 × 74) velocity vectors were obtained for a instantaneous velocity field at a rate of 15 frames. The number of particles in an interrogation area was in between 20 and 25. The uncertainty in velocity relative to depth averaged velocity is about 2% in the present experiments. The water was seeded with 12 μm diameter hollow glass sphere particles. Spurious velocity vectors (less than 3%) were removed using the local median-filter technique and replaced by using a bilinear least squares fit technique between surrounding vectors. The velocity vector field was also smoothed to avoid dramatic changes in the velocity field using the Gaussian smoothing technique. The vorticity value at each grid point was calculated from the circulation around the eight neighboring points.

3. Results and Discussions

Figure 3. shows time averaged velocity vector field <V> in the first column, Reynolds Shear stress contours in the second column and the streamline topology <ψ> in the third column respectively with yaw angles from α=0° to 45°, for the gap ratio G/D=0.25. It is observed that jet like flows occurs until the gap ratio reached to G/D=2.0 as one observed by Akilli et al. [1].

Velocity vector fields show that flip-flop flow is evident at all yaw angles. Direction of biased flow is changing from one cylinder to another. Wider wake region is obtained in the behind of the upper cylinder at α=0°, 30° and 45° while wider wake region is observed in the behind of lower cylinder due to the biased flow. This flip-flop behaviour of flow has not been clarified yet in the literature (Akilli et al. [1]. As seen from the velocity vector map, with the increasing the yaw angle the strength of the jet-like flow decreases significantly. Patterns of Reynolds Stress for selected yaw angles are given in the second column. The dashed lines and solid lines stand for the negative (clockwise) and positive (counter clockwise) Reynolds Stress contours. It is observed that the jet-like flow has asignificant effect on the far wake region. However, the jet like flow is effective on the near wake region. The distrubutions of the Reynolds stress contours are similar but as the yaw angle increased the peak magnitude of the Reybolds stress increases. In the third column of streamline patterns, shear layers are visible between the cylinders. It can be said that due to the flopping behaviour of the flow, large scale foci occurs in the far wake region of the cylinder. At yaw angle of α=0° small scale foci occurs at the base of the lower cylinder, while large scale of foci are present at the upper cylinder. At α=15°, the counter rotating large scale focis are present at the lower cylinder. In addition to this, a vortex and saddle

point is observed at the lower cylinder. At the upper cylinder base, the vortex at the clockwise direction is emerged. Streamline patterns of yaw angle of α=20° is similar to α=15° case. But the foci which appeared behind the lower cylinder shifts the direction to the clockwise and saddle point is dissappeared at this case. At yaw angle 30° behind the upper cylinder, two focis placed in tandem and a saddle point are present. Then large scale of foci are emerged away from the cylinders. Center of these foci points are not seen. Due to the narrow wake region of the lower cylinder, small scale counter rotating foci points and a saddle point are evident downstream region of the lower cylinder. At yaw angle of α=45° the large scale of foci are decreased in the size compared to the other yaw angles, there are four foci points are present at far wake region of the lower cylinder side. Likewise α=30°, in the near wake region of the upper cylinder a foci and a saddle point is present.

Figure 4. represents patterns of time averaged velocity vectors <V> in the first column, the vorticity contours <ω> in the second column and the streamline topology <ψ> in the third column respectively at yaw angles from α=0° to 45°, for the gap ratio of G/D=0.5. As seen in the first column, jet-like flow dominates on the flow structure downstream of cylinders for all the cases. However by increasing the yaw angle, the penetration of jet-like flow into wake region decrease gradually. In the second column, as very strong jet-like flow where between the cylinders dominates for all the cases, large scale of Reynolds stress clusters take place downstream of cylinders. As yaw angle increased, the positive and negative Reynolds stress contours decreases in the size since the penetration of jet-like flow decreases.

In the third column, large scale counter rotating foci are observed in the far wake region of the upper cylinder and small scale counter rotating foci in the near wake region of the lower cylinder. Similar to gap ratio of G/D=0.25, by increasing up to the yaw angle of α=45°, at the wider wake region of the downstream cylinder, large scale counter rotating foci both shrink and move away from the cylinders and a different flow structure is emerged behind the cylinders. At α=45°, large scale counter rotating foci are dissappeared in the far wake region of the lower cylinder. Three foci are observed in the wake region of the lower cylinder. Foci are dissappeared and a nodal point is appeared in the near wake region of the upper cylinder at α=45°. Time averaged velocity vectors <V> in the first column, Reynolds shear stress contours in the second column and the streamline topology <ψ> in the third column are depicted in Figure 5. respectively at yaw angles from α=0° to 45°, for the gap ratio of G/D=0.75. It is observed that obtained result from the this gap ratio are similar with the gap ratio of G/D=0.5. In the second column it is evident that as the gap ratio, Reynolds stress are elongating in streamwise direction and expanding in transverse direction at all yaw angles. This is due to the increasing of incoming flow from upstream region to the downstream side between the cylinders. On the other side, the dimensions of positive and negative Reynold Stress contours decreased by increasing the yaw angle α. As seen from the streamline topology as the yaw angle increased, wide of wake region the downstream cylinder decreases, large scale foci shrink and and new flow structure are apperead on the upstream side. After yaw angle of α=20° these large scale foci dissappear. Likewise other gap flows, in the deflected near wake region of the cylinder, as yaw angle increased, vortex structures become smaller and get closer to the cylinder base. Figure 6 represents patterns of time averaged velocity vectors <V> in the first column, time averaged Reynolds shear stress contours and the streamline topology <ψ> in the third column respectively at yaw angles from α=0° to 45°, for the gap ratio of G/D=1.0. At this gap flow bistable flow is dissappeared. But weak interactions are observed between the cylinders. As seen from the velocity vector map the cylinders behave as single cylinder. As the yaw angle increased, the size

of wake region of the cylinders decreases. In the second column the dimensions of positive and negative Reynold Stress contours decreased by increasing the yaw angle α. It can be said that, the scale of the Reynold stress contours changed as a function of yaw angle, for all gap ratios. As the yaw angle increased, Reynolds Stress contours decreases gradually due to the effect of the jet-like flow decrease, the contours of negative and positive Reynolds stress take place symmterical form. Streamline topologies depict that counter rotating symmetrical vortices emerged in the farwake region and the near wake region of the lower and upper cylinders at α=0° As increased the yaw angle, the scale of vortex structures decreases. At yaw angle of α=15°, two foci points is appeared in the wake region of the upper cylinder and a focus point is appeared in the near wake region of the lower cylinder. At yaw angle of α=20°, symmetrical vortex structures are observed in the wake region of the side-by-side cylinders. At yaw angle of α=30°, in the wake region of the upper cylinder, a foci in clockwise direction and another foci elongated in streamwise direction are observed, these foci are similar to yaw angle of α= 20°. In the wake region of the lower cylinder, foci are dissappeared and a nodal point is appeared instead of it. Elongated foci is decreased and gets close to the cylinder base. At α=45°, small scale foci and nodal points are observed in the wake region of the side-by-side cylinders.

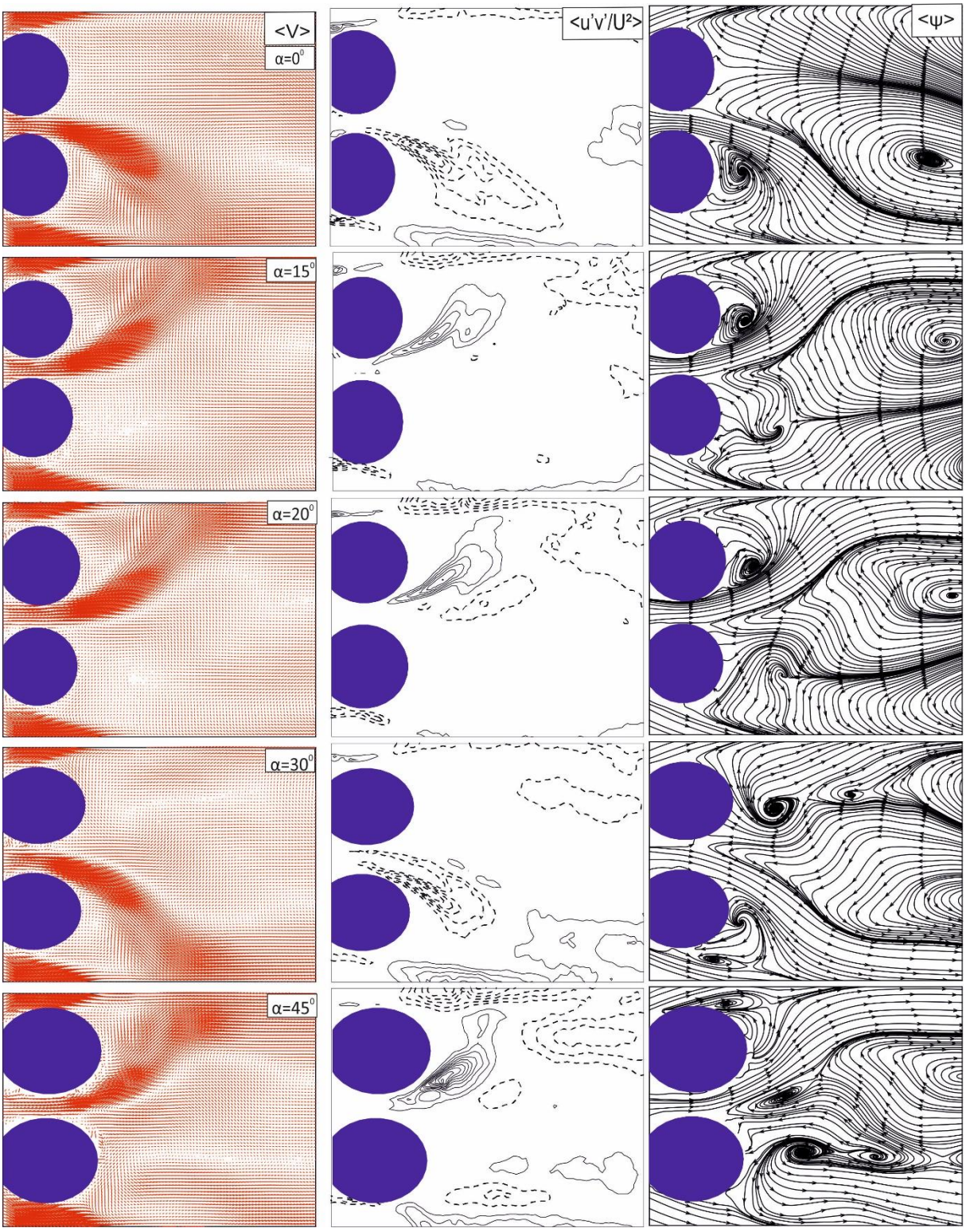

Figure 3. Time averaged velocity vector fields <V> , averaged Reynolds shear stress contours and corresponding time averaged streamline topology <ψ> for the gap ratio of G/D=0.25. Minimum and incremental values Reynolds shear stress are $[<u'v'>/U^2]_{min}=\pm 0.005$, $\Delta\,[<u'v'>/U^2]=0.005$

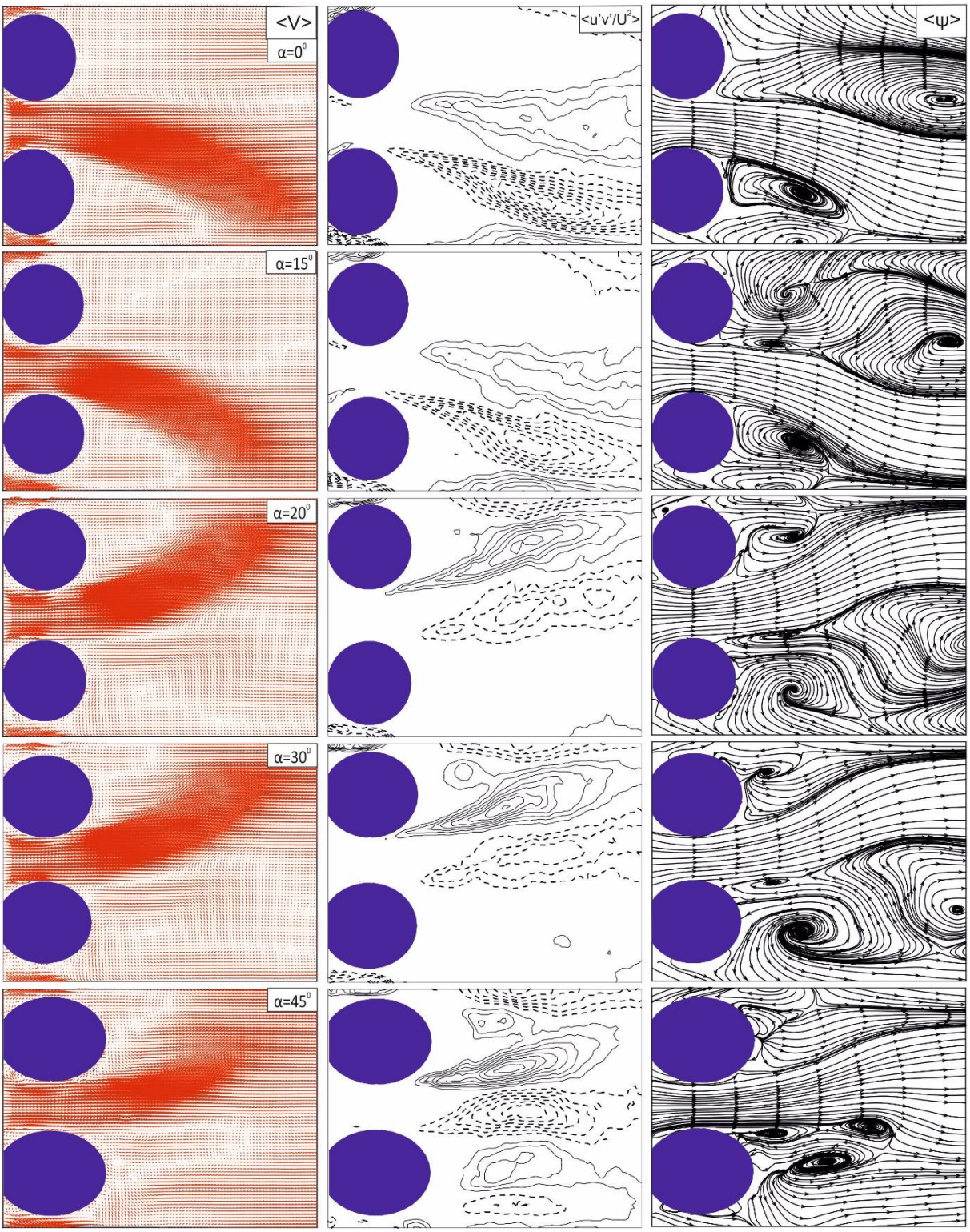

Figure 4. Time averaged velocity vector fields <V> , averaged Reynolds shear stress contours and corresponding time averaged streamline topology <ψ> for the gap ratio of G/D=0.5. Minimum and incremental values Reynolds shear stress are $[<u'v'>/U^2]_{min}=\pm 0.005$, $\Delta\,[<u'v'>/U^2]=0.005$

Figure 7. shows time averaged velocity vector field <V> in the first column, contours of Reynolds stress in the second column and the streamline topology <ψ> in the third column respectively at yaw angles from α=0° to 45°, for the gap ratio of G/D=1.25. At this gap flow the flow structures of the side-by-side cylinders are independent from the each other and cylinders are not affected by each others. However yaw angles are effective on each of the cylinders. Velocity vector fields and Reynolds shear stress contours indicates that with the increasing the yaw angle, wake region in the first column and Reynolds shear stress layers in the second column are getting smaller. In the third column, large scale of foci decrease as yaw angle increased.

Conclusions

This study illustrates the flow characteristics in the wake region of the two yawed side-by-side cylinders in shallow water conditions. Particle Image Velocimetry (PIV) method is employed to investigate flow patterns such as velocity vector fields, Reynolds shear stress contours and streamlines. The velocity vector fields illustrated that when increasing the yaw angle, the penetration of jet-like flow shrinks gradually for gap ratios of G/D=0.25, 0.5, 0.75. The intensity of negative and positive Reynolds shear stresses clusters growed as the gap ratio increased. On the other hand, the peak magnitude of the negative and positive Reynolds shear stress decrease as the yaw angle increased for each of gap ratios. Streamline topology of the flow demonstrated that, in the deflected near wake region of the cylinder, as yaw angle increased vortex structures become smaller and get close to the cylinder base. Also in the far wake region of the cylinder, large scale of the vortices shrink and new vortex structures are emerged on the upstream side. After gap ratio of G/D=1.75, the cylinders are not affected by each other. However as yaw angle increased; the wake region of the cylinders, Reynolds shear stress layers and counter foci decrease as a function of yaw angle α.

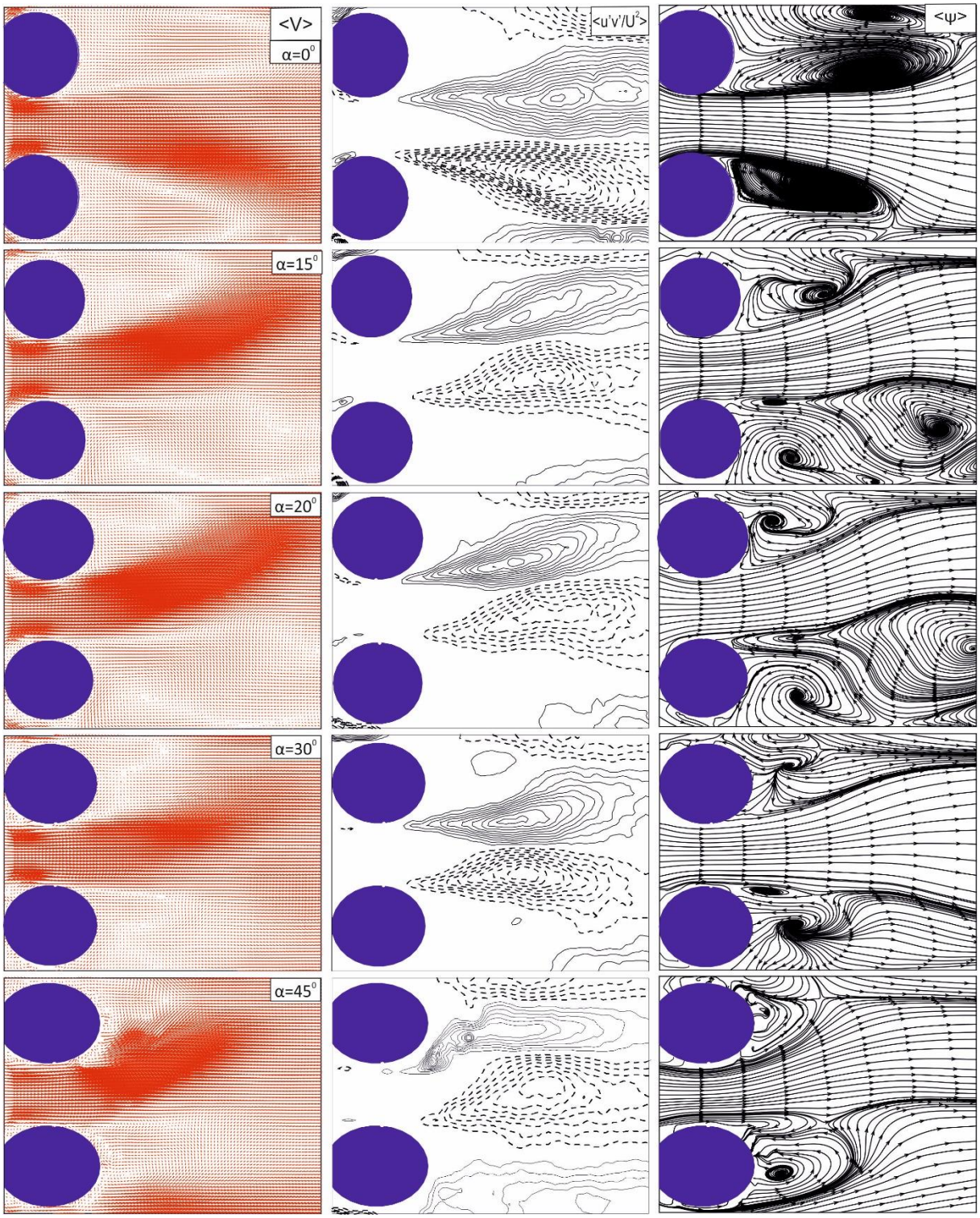

Figure 5. Time averaged velocity vector fields <V> , averaged Reynolds shear stress contours and corresponding time averaged streamline topology <ψ> for the gap ratio of G/D=0.75. Minimum and incremental values Reynolds shear stress are $[<u'v'>/U^2]_{min}=\pm 0.005$, $\Delta\,[<u'v'>/U^2]=0.005$

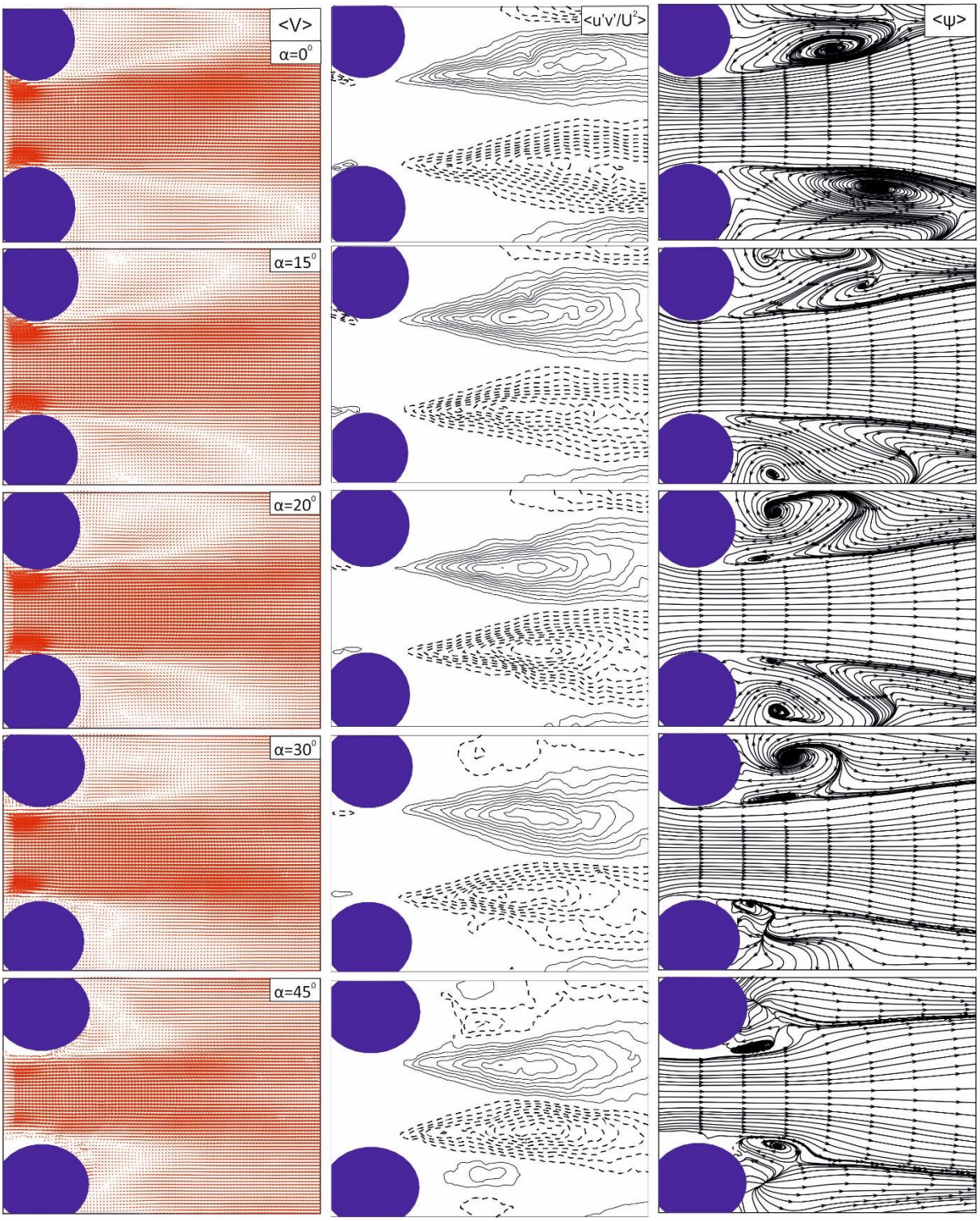

Figure 6. Time averaged velocity vector fields <V> , averaged Reynolds shear stress contours and corresponding time averaged streamline topology <ψ> for the gap ratio of G/D=1.0. Minimum and incremental values Reynolds shear stress are $[<u'v'>/U^2]_{min}=\pm 0.005$, $\Delta\,[<u'v'>/U^2]=0.005$

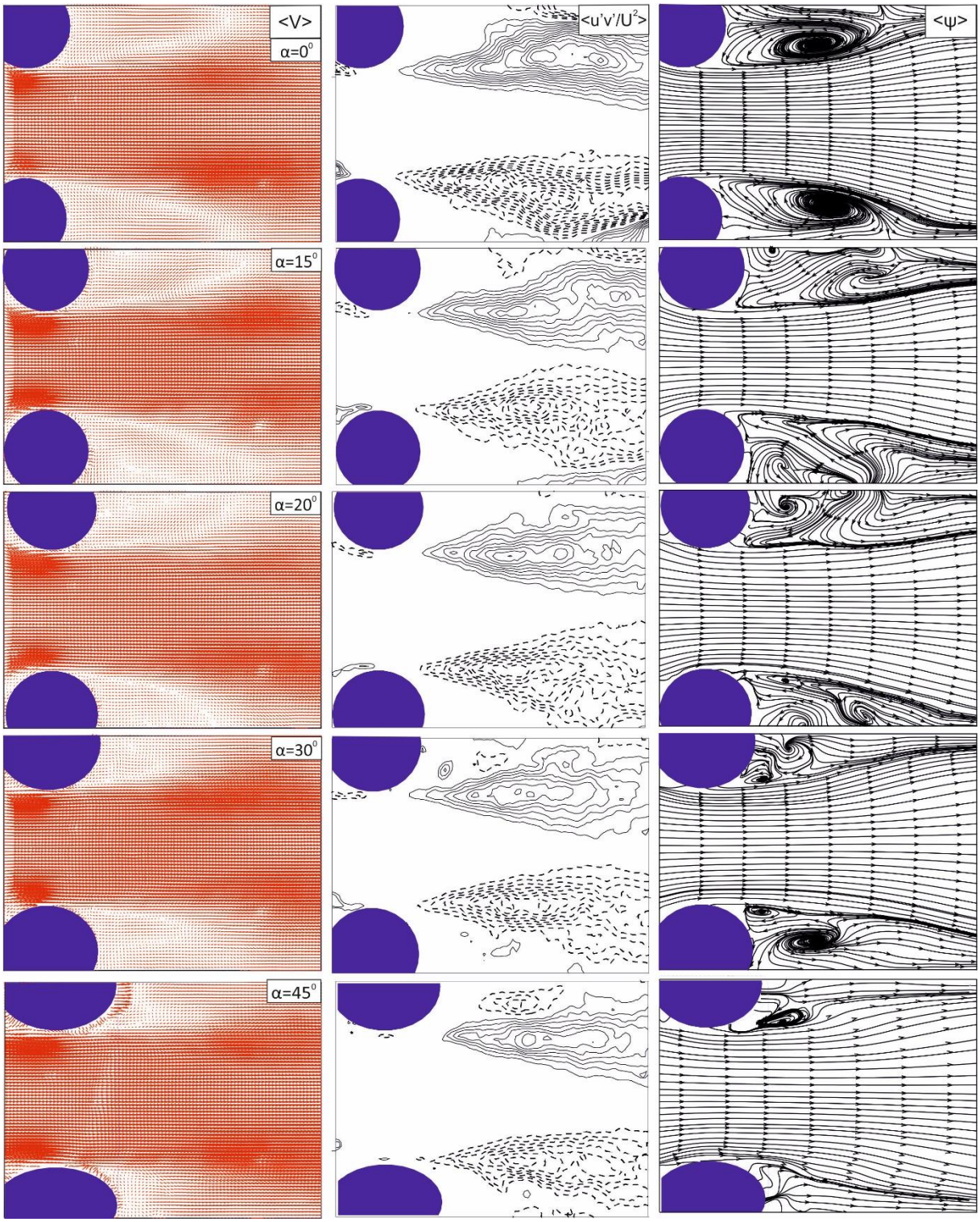

Figure 7. Time averaged velocity vector fields <V> , averaged Reynolds shear stress contours and corresponding time averaged streamline topology <ψ> for the gap ratio of G/D=1.25. Minimum and incremental values Reynolds shear stress are $[<u'v'>/U^2]_{min}=\pm 0.005$, $\Delta\,[<u'v'>/U^2]=0.005$

References

[1] Akilli, H., Akar, A., Karakus, C. Flow characteristics of circular cylinders arranged side-by-side in shallow water. Flow Measurement and Instrumentation 2004;15:187-197.

[2] Akilli, H.,Rockwell, D. Vortex formation from a cylinder in shallow water. Physics of Fluids 2002;14:2957–2967.

[3] Alam, M. M., Moriya, M., Takai, K., Sakamoto, H. Fluctuating fluid forces acting on two circular cylinders in a tandem arrangement at a subcritical Reynolds number. Journal of wind Engineering 2003;91:139-154.

[4] Bearman, P. W., and Wadcock, A.J. The interaction between a pair of circular cylinders normal to a stream. Journal of Fluid Mechanics 1973;61: 499-511.

[5] Chen, L., Tub, J. Y., and Yeoh, G. H. Numerical simulation of turbulent wake flows behind two side-by-side cylinders. J. Fluids Struct 2003;18(3), pp. 387-403.

[6] Franzini, G. R., Gonçalves, R. T., Meneghini, J., R., and Fujarra, A. L. C., Experimental investigation into the flow around a stationary and yawed cylinder under asymmetrical end conditions, Int. J. Offshore Polar Eng., 2014; 24(2), pp. 90-97.

[7] Hogan, J. The spanwise dependence of vortex-shedding from yawed circular cylinders. J. Pressure Vessel Technol 2010; 132(3), pp. 031301.

[8] Ingram, G. R. and Chu, V. H. Flow around islands in Rupert bay: an investigation of the bottom friction effect. Journal of Geophysical Research 1987;92 (C13), 14521-14533.

[9] Le Gal, P., Peschard, I., Chauve, M. P., Takeda, Y. Collective behaviour of wakes downstream of a row of cylinders. Physics of Fluids 1996;8: 2097-2106.

[10] Liang, H., Jiang, S. Y., Duan, R. Spanwise characteristics of flow crossing a yawd circular cylinder of finite length. Procedia Engineering 2015;(126) 83-87.

[11] Oruc, V., Akar, M. A., Akilli, H., Sahin, B. Suppression of asymmetric flow behaviour downstream of two side-by-side circular cylinders with a splitter plate in shallow water. Measurement 2013;46:442-455.

[12] Sumner, D., Wang, S. S. T., Price, S. J., and Paidoussis, M. P. Fluid Behavior of side-by- side circular cylinders in steady cross-flow. Journal of Fluids and Structures 1999; 13: 309-338.

[13] Thapa, J., Zhao, M., Zhou, T., and Cheng, L. Three-dimensional simulation of vortex shedding flow in the wake of a yawed circular cylinder near a plane boundary at a Reynolds number of 500. Ocean Eng 2014;87(9), pp. 25-39.

[14] Vakil A., and Green, S. I. Drag and lift coefficients of inclined finite circular cylinders at moderate Reynolds numbers. Comput. Fluids, 2009;38(9), pp. 1771-1781.

[15] Wei, C. Y., and Chang, J.R., Study of base-bleed flow and wake downstream of two dimensional bluff bodies arranged side by side, in: The Sixth Military Academy Symposium on Fundamental Science, ROC 1999.

[16] Williamson, C. H. K. Evolution of a single wake behind a pair of bluff bodies. Journal of Fluid Mechanics, 1985;159: 1-18.

[17] Zdravkovich, M. M., Review of flow interference between two circular cylinders in various arrangements. J. Fluid Eng. 1977;99(4), pp. 618-633.

[18] Zhou, Y., Wang, Z. J., So, R. M. C. S., Xu, J. and Jın, W. Free vibrations of two side-by-side cylinders in a cross flow,'' J. Fluid Mech. 2001;443, 197-229.